IEEE Access
Multidisciplinary | Rapid Review | Open Access Journal

Received 4 March 2024, accepted 4 April 2024, date of publication 11 April 2024, date of current version 19 April 2024.

Digital Object Identifier 10.1109/ACCESS.2024.3387535

TOPICAL REVIEW

On the Automated Unruptured Intracranial Aneurysm Segmentation From TOF-MRA Using Deep Learning Techniques

V. A. ANIMA AND MADHU S. NAIR, (Senior Member, IEEE)
Artificial Intelligence and Computer Vision Laboratory, Department of Computer Science, Cochin University of Science and Technology, Kochi, Kerala 682022, India

Corresponding author: V. A. Anima (animaarjun@gmail.com)

The research work is supported by the Kerala State Higher Education Council (KSHEC) under the Kairali Research Award 2020 Project. (File No: KSHEC-A3/352/Kairali Research Award/47/2022).

ABSTRACT Aneurysms pose a life-threatening risk due to weakened vessel walls, causing bulging or ballooning in arterial blood vessels. The growth of an aneurysm increases the risk of rupture and consequent bleeding in the brain, leading to a hemorrhagic stroke. Therefore, accurate detection and segmentation of intracranial aneurysms are crucial for treatment planning in patients. Recently, the use of Time of Flight Magnetic Resonance Angiography (TOF-MRA) for automated segmentation of intracranial aneurysms has gained significant importance. This study comprehensively evaluates different automated segmentation methods for unruptured intracranial aneurysms, using the publicly available Aneurysm Detection and Segmentation (ADAM) challenge dataset. The performance and method scalability of these methods is analyzed across state-of-the-art algorithms, and the experimental analysis shows that 3D U-Net architecture outperforms in the segmentation tasks.

INDEX TERMS Aneurysm, computer-aided detection, time of flight-magnetic resonance angiography, unruptured intracranial aneurysm, dice similarity coefficient.

I. INTRODUCTION

A cerebral aneurysm is a condition where an arterial vessel bulges or balloons, which can gradually increase in size and potentially lead to rupture. If a rupture does occur, it can cause severe bleeding in the brain, resulting in a hemorrhagic stroke. Unfortunately, studies have shown that approximately one-third of those affected do not survive and survivors may experience long-term movement disabilities [1]. Aneurysms can vary in size and shape and may not cause any symptoms initially. However, if an aneurysm ruptures or leaks, it can lead to serious and potentially life-threatening consequences [2]. Therefore, it is critical to prevent and detect aneurysms before they rupture. Health professionals rely on various imaging techniques to estimate the aneurysm's size, location and morphological characteristics to aid in early detection and prevention [3].

The associate editor coordinating the review of this manuscript and approving it for publication was Luca Cassano.

Digital Subtraction Angiography (DSA), Computer Tomography Angiography (CTA) and Magnetic Resonance Angiography (MRA) are the most commonly used imaging techniques to examine aneurysms [4]. However, DSA and CTA techniques are invasive in nature and require the use of contrast agents during the diagnosis procedure. Thus, a non-invasive and non-contrasting imaging technique is recommended for earlier detection and aneurysm prediction in routine clinical environments. MRA is the widely accepted non-invasive technique for medical image analysis, which can be used to identify Unruptured Intracranial Aneurysms (UIAs). MRA utilizes the magnetic resonance property of electromagnetic waves to generate imaging sequences and represent them as two-dimensional or three-dimensional structural images.

Time Of Flight - MRA can detect aneurysms by monitoring the hemodynamic flow in the arterial vessel structure, which captures the blood flow within the vessel structure. These characteristics of TOF-MRA make it a suitable candidate

for detecting aneurysms. However, clinicians face difficulties in analyzing the TOF-MRA sequence for aneurysms due to its complex morphological features. As a result, manual processing of TOF-MRA is time-consuming and a hectic task for radiologists in their busy schedules [5].

To reduce the reading time of the MRA sequence, technicians have employed the Maximum Intensity Projection (MIP) representation of the sequence for the monitoring process, thereby reducing the overall time of the diagnosis procedure. Unfortunately, this representation is vulnerable to noise and may lead to the disappearance of small-sized aneurysms. Therefore, there is a necessity for computer-aided detection (CAD) of cerebral aneurysms in clinical diagnosis to enhance the performance of an aneurysm prevention system. CAD systems can assist clinicians in reading the TOF MRA volume, thereby reducing the workload and improving the efficiency of clinical diagnosis.

Before the rapid growth of machine learning (ML) and deep learning (DL) techniques, CAD systems for cerebral aneurysm detection followed traditional approaches. These traditional methods relied on domain-specific features for the decision-making process. Specifically, CAD systems extracted relevant aneurysm features from TOF-MRA using various filtering approaches. However, with the rise of ML and DL techniques, CAD systems can now utilize advanced algorithms to extract features automatically and accurately, improving the performance of the system.

The management of intracranial aneurysms mainly rely on artificial inteligence from 2015 onwards. Artificial Inteligence (AI) can identify a likely diagnosis and select a suitable treatment based on health records or imaging information without any explicit programming [6], [7], [9]. Detecting brain aneurysms can be tricky and take a lot of time, leading to potential misdiagnoses. Artificial intelligence (AI) tools, specifically computer-assisted diagnosis (CAD), could offer a solution. These AI-powered tools, fueled by machine learning, are showing promise as diagnostic biomarkers, meaning they can help identify aneurysms accurately and efficiently [8], [10].

This article presents a comparative analysis of various automated segmentation methods for unruptured intracranial aneurysms using the publicly available Aneurysm Detection and Segmentation (ADAM) challenge dataset. The study includes quantitative and qualitative experiments to analyze the performance of these methods across TOF-MRA modalities, providing valuable insights for guiding the diagnostic and treatment processes of aneurysms. The primary objective of this study is to evaluate the effectiveness of different automated segmentation techniques for the detection of cerebral aneurysms and to determine the most accurate and reliable method for clinical diagnosis. This research aims to contribute to the development of an accurate, efficient and non-invasive CAD system that can assist clinicians in the diagnosis and treatment of cerebral aneurysms.

The main observations of this research is outlined below:

- As per the review, we observe that detecting and segmenting small aneurysms poses a significant challenge for current architectures, potentially resulting in under-detection and impacting the effectiveness of CAD systems in routine clinical settings.
- Based on our empirical analysis, it is evident that while the current CAD system excels in detecting large aneurysms, it occasionally faces challenges in precisely determining the shape and morphological attributes of identified aneurysms.
- The study highlights the crucial role of precise segmentation in assessing the rupture risk of unruptured intracranial aneurysms, emphasizing the intricate relationship between the shape and morphological attributes of aneurysms and their risk estimation.
- It has been observed that the current 2D U-Net architectures sometimes fail to capture essential topological information across slices in TOF-MRA volumes, treating slices independently for detection and segmentation tasks. This limitation may compromise CAD model efficiency and accuracy.
- Experimental results shows that the U-Net model's encoder-decoder structure may lead to overfitting, requiring abundant training data or regularization techniques. Yet, the medical domain faces a challenge in acquiring sufficient training data for model generalization. Addressing data scarcity is vital for developing an effective CAD model.
- It has been observed that current segmentation models are typically resource-intensive, imposing significant computational demands. This highlights the necessity for a lightweight model in the task of aneurysm detection and segmentation.

II. METHODS

The detection and segmentation of UIAs can be classified into two categories: traditional methods and deep learning-based methods. This article focuses on the identification and separation of aneurysms, specifically using TOF-MRA images, without incorporating techniques from other imaging modalities. Figure 1 presents a generic framework for automated unruptured intracranial segmentation from TOF-MRA images based on existing methods. The framework comprises three main steps: (1) pre-processing (2) aneurysm segmentation and (3) post-processing. Since TOF-MRA images have varying intensities and shades, a pre-processing module is included to enhance and equalize image quality. Additionally, a post-processing step is implemented to reduce false positive regions. This work standardizes existing automated UIA segmentation methods using the workflow illustrated in Figure 1.

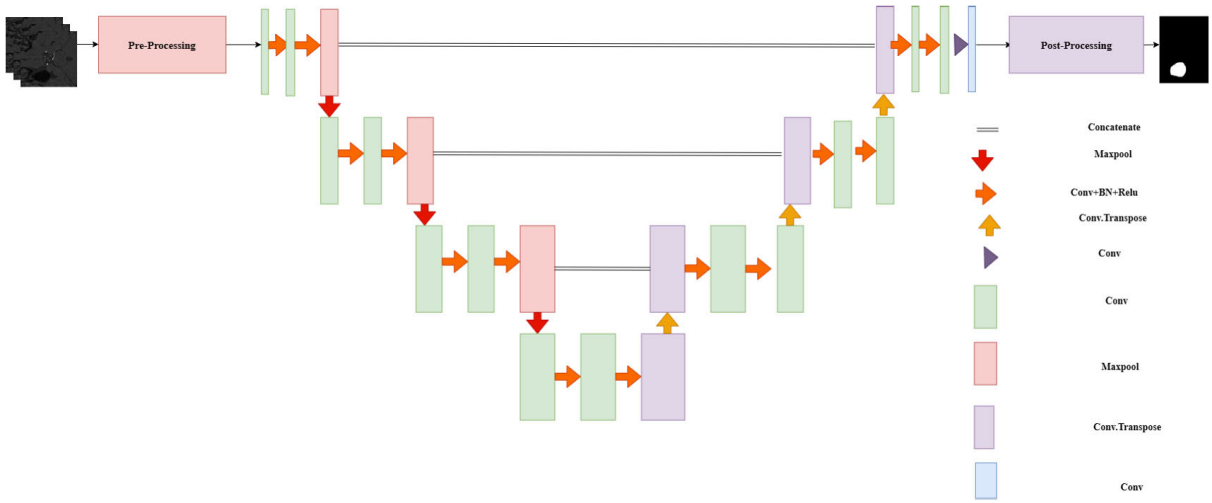

FIGURE 1. General framework for unruptured intracranial aneurysm segmentation system.

A. TRADITIONAL METHODS FOR ANEURYSM DETECTION AND SEGMENTATION

This section discusses the traditional methods that have been proposed for the segmentation of intracranial aneurysms prior to the advent of deep learning techniques. These methods include both fully automated and semi-automated approaches which require some user interactions. Some of these methods make use of machine learning techniques with handcrafted features, while others involve pre-processing and filtering to detect or segment aneurysms.

Several methods have been proposed for the segmentation and detection of aneurysms in medical imaging. Firouzian et al. [11] proposed a semi-automatic segmentation method for the detection of aneurysms in CTA images. The method utilizes Geodesic Active Contours (GAC) implemented through the level-set framework, where a surface is evolved to capture the aneurysm. The method starts from a single user-defined seed point and grows from there. Bogunović et al. [12] presented an automatic multimodal segmentation technique that uses Geodesic Active Regions and a deformable model within the level-set framework. This method also combines region-based descriptors with gradient ones to guide the evolution towards vascular boundaries. Sen et al. [13] proposed a Threshold-Based Level Set (TLS) method for segmenting aneurysms. TLS combines GAC and the Chan and Vese model [14] within the level-set framework and merges both region and boundary information. The method uses a global threshold and gradient magnitude to form the function that evolves the segmentation towards the cerebral aneurysm. The Chan-Vese model computes the initial threshold value, which is iteratively updated throughout the segmentation process. Sunaiga et al. [15] proposed an automatic detection and localization method for aneurysms from the TOF-MRA dataset. The method involves computing the 3D centerline from the extracted cerebrovascular segmentation, followed by classification of initial aneurysm candidates using Support Vector Machine (SVM) based on extracted parameters like 3D Forstner filter.

In addition, Yang et al. [16] proposed an algorithm that involves segmenting the cerebral vasculature in the first step and then finding candidate regions of different kinds of Points Of Interest (POI) using different techniques. A small set of suspicious POIs is chosen from the whole POIs and a probability score is assigned based on the likelihood of representing the aneurysm. The suspicious POIs are then ranked in descending order of probability score and clusters of POIs are blended to eliminate overlapping detections.

B. DEEP LEARNING-BASED ANEURYSM DETECTION AND SEGMENTATION

This section provides an overview of deep learning-based methods used for aneurysm segmentation. Traditional methods require manual intervention to select handcrafted engineering features. These features are then fed into the models trained for classification, detection or aneurysm segmentation. However, deep learning algorithms can automatically learn features from the data, leading to improved results in radiology. In particular, deep learning algorithms have become the most promising tool for intracranial aneurysm management, as they are not only used for detecting UIAs but also for estimating the rupture risk and predicting treatment outcomes.

Stember et al. [17] introduced a deep learning approach based on the U-Net [18] architecture for detecting and segmenting cerebral aneurysms on TOF-MRA images. The proposed method consists of two main steps. Firstly, aneurysm images with a resolution of 256×256 are fed into a 20-layer U-Net model, which is specifically designed for medical image segmentation. The U-Net is a convolutional neural network architecture that includes contracting and expanding paths as well as a connection path that merges features from both paths. This combination of

paths enables the model to effectively capture and utilize information from multiple scales of the input image. The training process involves iteratively performing forward and backward propagation. During forward propagation, input images are fed into the network, resulting in perpixel likelihood predictions as output. The backpropagation process uses the steepest gradient descent method and the Adam optimization algorithm to update parameter values and is run iteratively for up to 60 epochs. The initial weight is randomly chosen with a mean of zero and the learning parameters are automatically tuned. By adjusting the threshold value, a predicted pixel group or cluster can be created.

Sichtermann et al. [19] proposed a deep learning-based approach for detecting intracranial aneurysms in 3D TOF-MRA images. The authors used their own dataset of patients with a history of one untreated intracranial aneurysm, which was collected between 2015 and 2017. Before feeding the images into the deep learning model, the authors performed several pre-processing steps including voxel size resampling ($0.5 \times 0.5 \times 0.5$), intensity normalization to a zero mean unit variance space, skull stripping using BET2 [20] and N4 bias field correction [21]. The authors then utilized the Deep Medic framework to segment the aneurysms. The Deep Medic network consists of two identical pathways, with the input to the second pathway being a subsampled version of the first. They uses three dimensional convolution operations followed by max pooling layers. The convolutional layers extract features from the input image, while the max pooling layers reduce the dimensionality of the output. The architecture also includes a number of skip connections, which allow information to flow directly from the earlier layers of the network to the later layers. This helps to preserve fine-grained details in the segmentation. The authors used a learning rate of 0.001, which was gradually reduced and set a Nesterov Momentum of 0.6 for optimization. In order to enhance regularization, the researchers incorporated dropout and applied L1 regularization with a value of 0.000001 and L2 regularization with a value of 0.0001. Additionally, the authors used ReLU activation functions and batch normalizations as implemented in the Deep Medic framework to accelerate the convergence of the model.

Claux et al. [22] presented a two-stage regularized U-Net approach for the detection of intracranial aneurysms in TOF-MRA images using deep learning. The authors used a dataset from the radiology department, consisting of confirmed cases of unruptured saccular aneurysms. The U-Net [18] network model was employed with two folds. In the first network, vessel segmentation was performed and the output was fed into the second network, which detected aneurysms using only the topological information of the binary data produced. The Adam optimizer was used for the training process. The segmentation stage of the model uses a regularized U-Net model to segment the intracranial arteries in the TOF-MRA image, which helps to improve the robustness of the model to noise and artifacts. The detection stage of the model uses a two-stage U-Net model to detect aneurysms in the segmented intracranial arteries, which helps to improve the accuracy of the model. This architecture is also complex and require more computational resources and needs much time for training.

Di Noto et al. [23] introduced a deep-learning model for segmenting UIAs. The method involves various pre-processing steps such as skull stripping using the FSL Brain Extraction tool (v 6.0.1) [20], N4 Bias field correction with SimpleITK (v 1.2.0) [21] and resampling all volumes to a median voxel spacing with SimpleITK to normalize non-uniform voxel sizes. Moreover, they utilized a probabilistic vessel atlas constructed from multi-center MRA datasets. In this method the authors utilized the weak labels, which are faster and much more easier to generate than the voxel-wise labels. This method also integrates anatomical knowledge into the model, which helps to focus on the most likely locations for aneurysms. This can remarkably improve the model's accuracy and reduce the number of false positives. During training procedure, this method combines the weak and voxel-wise labels which also helps to improve the model's performance.

Yunqiao et al. [24] put forth a segmentation technique for UIAs that relies on deep learning. Specifically, they utilized a 3D U-Net model that underwent minor modifications, such as substituting Batch Normalization with Group Normalization and replacing ReLU with Leaky ReLU. Additionally, they integrated Dice ranking to enhance the accuracy of small lesion segmentation. It utlizes 3D U-Net ensemble method for aneurysm segmentation, inorder to avoid overfitting and adversarial effects of noise, here ensembles multiple 3D U-Net models are trained with a different data augmentation strategy. This method is not prone to overfitting since various data augmentation techniques applied and improves the robustness of the model.

C. POPULAR DEEP LEARNING ARCHITECTURES FOR SEGMENTATION

This section describe some of the popular deep learning architectures for segmentation task.

1) ATTENTION U-Net

Attention U-Net [25] used attention mechanism to the underlying U-Net architecture that allows the U-Net to focus on the target structures of varying size and shape. The attention mechanism in Attention U-Net is implemented as an attention gate. The attention gate takes two inputs: the feature map from the current layer and the feature map from the previous layer. The attention gate then computes a weight for each pixel in the feature map from the current layer, based on how well that pixel matches the feature map from the previous layer. The weighted feature map is then used as input to the next layer of the network.

The Attention U-Net applies attention to the feature maps extracted from the contracting path to focus on specific regions of interest. This helps to address the limitation of U-Net, which can miss local details, and achieve more

accurate segmentation results. The attention mechanism pays attention to the features extracted from contracting path,which assigns weights to specific regions of interest, allowing the model to focus on those regions.

2) ResUNet

ResUNet [26] is a fully convolutional neural network (FCN) architecture that combines the advantages of U-Net and residual neural networks (ResNets). It is one of the efficient method for medical image segmentation. Residual blocks allow the network to learn more complex features without the problem of vanishing gradients. The ResUNet [26] architecture consists of an encoder and a decoder, just like the U-Net architecture. The encoder is responsible for extracting features from the input image and the decoder is responsible for reconstructing the image from the extracted features. The residual connections are added between the encoder and decoder, which helps to improve the flow of information between the two parts of the network. ResUNet incorporates residual blocks into contracting and expanding paths. Residual blocks allow the network to learn more complex relationships between features at different layers, without the problem of vanishing gradients. ResUNet also uses skip connection in this architecture, which makes it access features from all layers of the network, which allows the network to learn the context of each pixel in the image. This architecture takes the advantage of both the U-Net architecture and deep residual learning. Residual connections are a way of bypassing some of the layers in a neural network, which can help to prevent the network from overfitting and to improve its performance.

3) ResUNet++

ResUNet++ [27] is an extension of ResU-Net architecture, designed to address some of its limitations while improving the accuracy of image segmentation tasks. ResUNet++ incorporating several additional modules to enhance it's performance. These modules include residual blocks, squeeze and excitation blocks, atrous spatial pyramid pooling (ASPP) and attention blocks. Residual block is used to mitigate the vanishing gradient problem by introducing shortcut connections that skip over the intermediate layers. The squeeze and excitation block dynamically adjust the feature weights based on their channel-wise significance, which help the network to focus on the most relevant features leading to an optimal feature extraction and representation. The ASPP module captures multi-scale contextual information by applying convolutions with different dilation rates to the feature maps. This enables the network to capture both fine-grained and global contextual information, which is crucial for accurate semantic segmentation. And, the attention blocks are used to emphasize on the most relevant parts of the image to extract the relevant features.

ResUNet++ also includes dense bridge connections and multi-scale outputs. Dense bridge connections connect the corresponding encoder and decoder blocks at different scales. This allows the network to learn long-range dependencies between features at different scales. Multi-scale outputs allow the network to produce segmentation masks at different scales, which can be useful for improving the accuracy of segmentation for small objects. ResUNet++ also requires less computing resources than the 3D U-Net architectures.

4) SegAN

SegAN [28] make use of the concepts Generative adversarial training Networks [41]. SegAN (Segmenting Generative Adversarial Network) is a deep learning architecture for image segmentation that combines the benefits of generative adversarial networks (GANs) and convolutional neural networks (CNNs). The SegAN architecture consists of a Generator and a Discriminator. The generator network is responsible for producing segmentation masks, while the discriminator network is responsible for distinguishing between real segmentation masks and fake segmentation masks generated by the generator network [41]. Both these components trained in an adversarial manner. SegAN is more robust to noise and occlusion than traditional CNN-based segmentation methods. This is because the generator network in SegAN is trained to learn the distribution of real segmentation masks, which includes a variety of noise and occlusion patterns. This method requires more computtional power and time for training. It is particularly well-suited for image segmentation tasks where the images are noisy or occluded.

5) nnU-Net

The nnU-Net [29] is a versatile deep learning model designed for biomedical image segmentation. It automatically adjusts pre-processing, network architecture selection, training and post-processing steps and selects between 3D U-Net, 2D U-Net, or a hybrid of both based on dataset properties. Its self-configuring mechanism eliminates the need for manual hyperparameter tuning, making it more user-friendly and efficient. Despite its name suggesting a new neural network architecture, nnU-Net stands for ''No New Net,'' emphasizing its focus on automating the segmentation framework rather than introducing a novel network design. Its hierarchical architecture, featuring U-Net structures at multiple levels, integrates multi-scale information for precise segmentation of biomedical images with diverse structures and scales.

The nnU-Net employs a comprehensive training and evaluation approach, integrated techniques like data augmentation, model ensembling, and cross-validation to enhance performance and generalization across various datasets. Its automatic design framework encompasses fixed, rule-based, and empirical parameters. Initially, constant decisions are optimized collectively, such as selecting an architecture template. Then, heuristic principles establish relationships between design and dataset attributes, with remaining choices

determined empirically from training data, forming the basis of nnU-Net's development.

III. EXPERIMENTS

A. DATASET

The work comparatively analyzes the performance of existing deep learning models on the publicly available Aneurysm Detection And segMentation (ADAM) dataset [30]. The dataset used in this study includes 3D TOF-MRA images, which consist of 113 training cases. These cases are composed of 93 volumes that contain at least one untreated and unruptured aneurysm, consisting of 35 baselines and 35 follow-up volumes of the same subject and 23 volumes from unique subjects. Additionally, the dataset includes 20 volumes without intracranial aneurysms.

The median age of subjects with UIAs (53 subjects) was 55 years, with 75% of the subjects being female. The images have undergone bias field correction to address any intensity non-uniformities. The N4 bias correction algorithm has been utilized for this purpose, effectively correcting low-frequency intensity variations in the MRA images [21]. The aneurysm label image is labeled as follows: background is represented by 0, the untreated and unruptured aneurysm is represented by 1 and the treated aneurysms or artifacts resulting from treated aneurysms are represented by 2. As the primary objective of this study is to automatically detect or segment untreated, unruptured aneurysms, label 2 is not necessary and is excluded from the evaluation process.

Fig. 2 and Fig. 3 shows the 2D slice and MIP representation of TOF-MRA samples from the dataset that contains normal TOF-MRA of the brain, a normal TOF-MRA pre-processed image, TOF-MRA with aneurysm and a TOF-MRA image with untreated and treated aneurysms. The brighter region shows the presence of an aneurysm.

B. EVALUATION METRICS

In this study, the performance of automated methods for segmenting and predicting aneurysms is quantitatively analyzed by comparing them with manually annotated ground truth (GT) region images. In this work, we perform segmentation of unruptured intracranial aneurysms followed by the evaluation of the number of True Positives (TP), False Positive (FP) and False Negative (FN) regions [31]. To evaluate the automated segmentation, the algorithm's output is compared with the ground truth data. True positives refer to the aneurysm regions that are correctly identified by the algorithm, while false positives are non-aneurysm regions that are incorrectly detected as aneurysms. False negatives are actual aneurysms that are not detected by the automated algorithm. The performance of the algorithm is measured in terms of precision and recall. Precision and Recall can be computed as in equation 1 and equation 2, respectively.

$$Precision = \frac{TP}{TP + FP} \tag{1}$$

$$Recall = \frac{TP}{TP + FN} \tag{2}$$

The Dice Similarity Coefficient (DSC) and Intersection over Union (IoU) are used to analyze the correlation of automated segmentation vs Ground Truth per each patient volume. The Dice Similarity Coefficient (DSC) is a statistical measure that quantifies the similarity between two sets of data. The DSC value ranges from 0 to 1, where a value of 1 indicates a perfect match between the two sets of data. The DSC can be computed as in equation 3,

$$DSC = \frac{2 * TP}{2 * TP + FP + FN} \tag{3}$$

The Intersection Over Union(IoU) is a measure of similarity between two sets of data. The value of the IoU ranges from 0 to 1, with 1 representing a perfect match and 0 representing no similarity between them. IoU can be computed as in equation 4,

$$IoU = \frac{TP}{TP + FP + FN} \tag{4}$$

We have also used the metrics such as Volumetric Similarity (VS) [32] and the Modified Hausdroff Distance (MHD) 95^{th} percentile to analyze the shape and structure of the aneurysms. VS is a metric used in 3D medical image segmentation tasks to assess the similarity between the segmented volume and ground truth volume. The value lies in between 0 and 1, 0 represents no similarity and 1 indicated the perfect similarity. VS can be computed as in equation 5,

$$VS = 1 - \frac{|FN - FP|}{2TP + FP + FN} \tag{5}$$

The modified Hausdorff distance (MHD) is a metric commonly used in medical image to measure the shape of segmentation. This is crucial because the shape can be used to gauge the risk of rupture when segmenting UIAs. MHD is used in segmentation to quantify the similarity between two sets of points or regions in 3D space. It measures the maximum distance of a point in one set to the closest point in the other set, and vice versa, providing a measure of the dissimilarity between the two sets. MHD provides a measure of the maximum distance between the points in two sets, capturing the spatial dissimilarity between them [42]. MHD can be computed as in equation 6, where A and B represents segmented volume and ground truth volume and $d(a, b)$ represents distance between points a and b.

$$MHD(A, B) = \frac{1}{|A|} \sum_{a \in A} \min_{b \in B} d(a, b) + \frac{1}{|B|} \sum_{b \in B} \min_{a \in A} d(a, b) \tag{6}$$

C. EXPERIMENTAL SETUP

Experimental analysis of the existing methods described in the previous section is performed on the TOF-MRA images from ADAM dataset. For each method described in Section II, the automated segmentation model follows a thresholding mechanism. The deep learning-based segmentation methods are implemented in TensorFlow 2 on a GPU server installed in Lenovo ThinkSystem SR670 with the

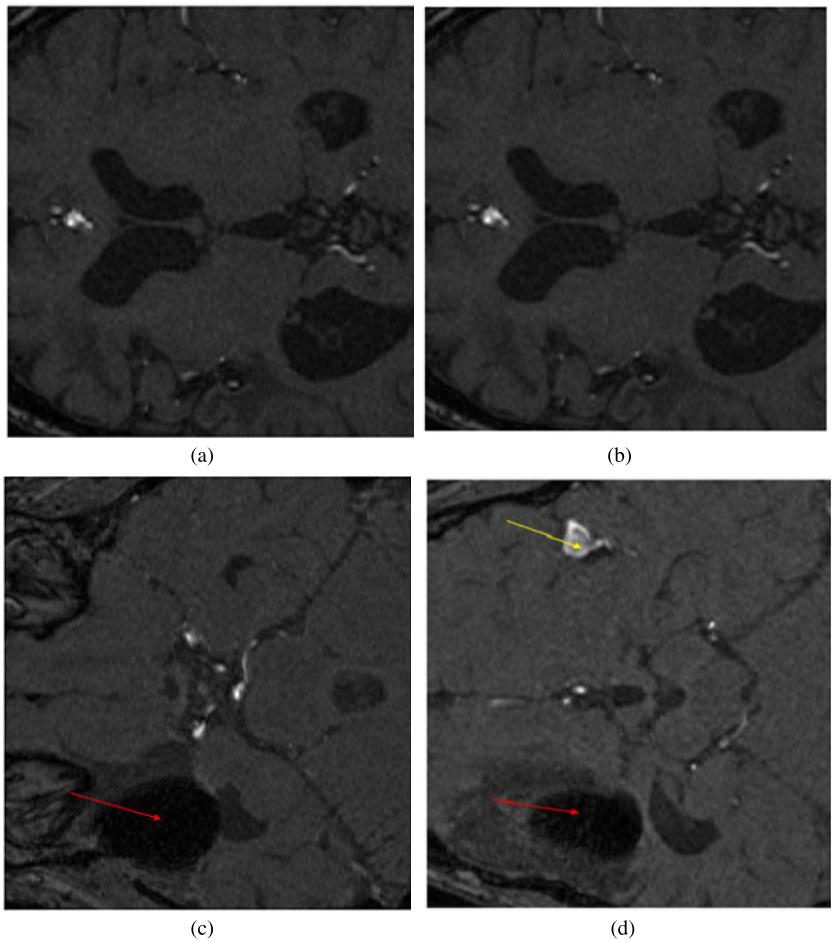

FIGURE 2. TOF-MRA images of ADAM dataset: (a) Normal TOF-MRA original (b) Normal TOF-MRA preprocessed (c) TOF-MRA with aneurysm (d) TOF-MRA with untreated aneurysm & treated aneurysm. (Yellow-colored arrow shows treated aneurysms and the red-colored arrow shows untreated aneurysms.)

following specifications: GPU card: 2* NVDIA A100 4OGB PCIe 4.0 CUDA Core 2*6912, Tensor core 2 *432. The Lenovo ThinkSystem sr670 has a processor 2* Intel Xeon Gold 6226R 16C 150 W 2.9 GHz and is composed of Memory 12*64GB DDR4 2933 MHz RDIMM with OS Ubuntu 20.04.

In the literature, it is evident that certain methods are tailored for application on 2D images, while others are designed for 3D volumes. Following this trend, we adopted a similar approach. We extracted 2D Maximum Intensity Projection (MIP) images from the volume and applied the models accordingly. Conversely, for methods designed for volume application, we directly input the volume without further manipulation.

D. PRE-PROCESSING

The study implemented a pre-processing technique for all TOF-MRA images to address the subjectivity of noise in Maximum Intensity Projection (MIP). Specifically, we utilized the N4 bias field correction algorithm, a widely used technique for correcting low-frequency intensity non-uniformity in MRI image data [21]. To reduce the size and complexity of the image, we applied a shrink factor. The N4 algorithm employs a multi-scale optimization technique to compute the bias field. We also used the ''Set Maximum Number Of Iterations'' [21] method, which limits the number of iterations per resolution level, effectively determining the number of scales and iterations. It's important to note that this filter requires a single input image that has been impacted by the bias field that we intend to rectify. After pre-processing, inorder to standardize every method we have extracted the non overlapping patches of size $64 \times 64 \times 64$ from the TOF-MRA volume. Then normalize each patches using Z-score normalization techniques [31].

IV. RESULTS AND ANALYSIS

In this section, we compare various automated deep learning-based UIA segmentation methods using quantitative metrics. Based on our study, the ideal method for segmenting unruptured intracranial aneurysms is one that demonstrates high precision and recall values. A low precision value suggests over-detection, while a low recall value suggests under-detection. Therefore, we emphasize the importance of achieving a balance between precision and recall when evaluating these segmentation methods.

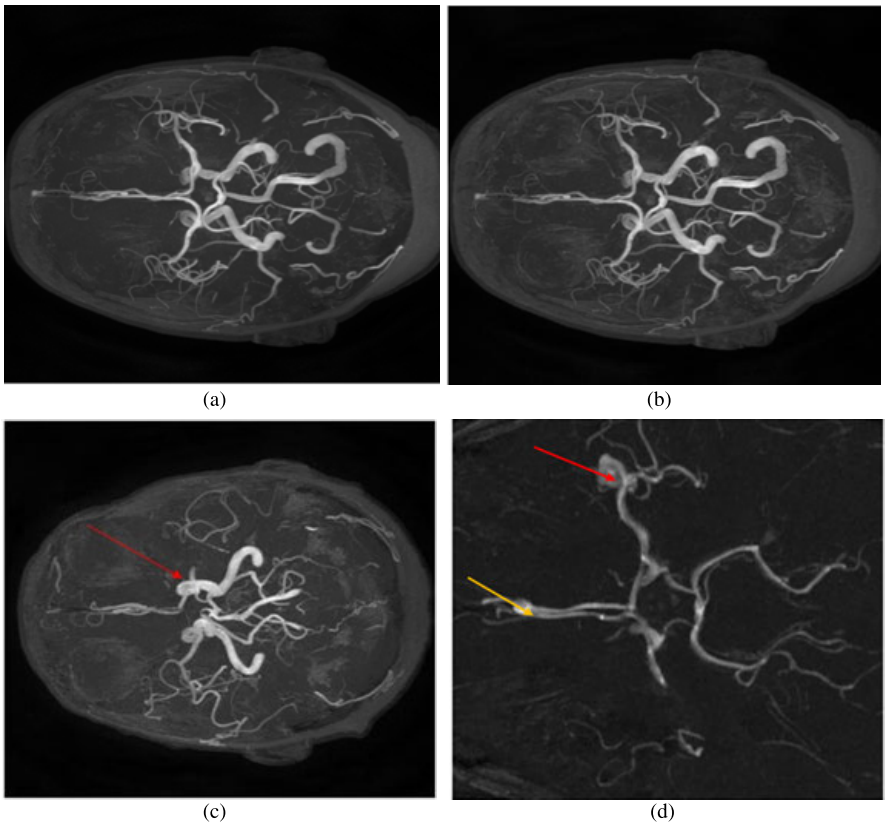

FIGURE 3. TOF-MRA Images of ADAM dataset with MIP representation: (a) Normal TOF-MRA original (b) Normal TOF-MRA preprocessed (c) TOF-MRA with aneurysm (d) TOF-MRA with untreated aneurysm & treated aneurysm. (Yellow-colored arrow shows treated aneurysms and the red-colored arrow shows untreated aneurysms.)

In the methods described, the authors have employed data augmentation techniques to expand the dataset by applying various operations to the input data. These operations include contrast enhancement, rotation, scaling and flipping. This is done to improve the model's ability to generalize and perform well on a wider range of inputs. The dice loss [39], which is used as the loss function in the above-mentioned methods, is a quantitative metric that assesses the similarity between predicted and actual data [42]. The dice loss quantifies the overlap between predicted and ground truth data.

Table 1 depicts the precision, recall, Dice Similarity Coefficient (DSC) and Intersection over Union (IoU) for the methods under analysis against the ADAM dataset. In terms of recall, the Di Noto et al. [23] method has exhibited superior performance compared to other automated methods, as per our study. Figure 6 represents the comparative analysis of existing deep learning methods based on precision and recall, and Figure 7 represents the comparative analysis of precision and recall of existing deep learning methods based with MIP representation of TOF-MRA volume.

Table 2 presents the performance analysis of existing models with MIP representation of TOF-MRA volume. It is evident from Table 2 that the method suggested by Stember et al. [17] outperforms all other 2D methods in terms of every metric. Qualitative evaluation of aneurysm segmentation on a sample TOF-MRA is presented in Fig. 4 and the corresponding MIP representation is in Fig. 5. From the qualitative analysis given in Fig. 4 and Fig. 5, it is evident that the 2D method proposed by Stember et al [17] and the 3D architecture proposed by Di Noto et al almost preserve the accurate size and shape during segmentation. From the analysis, it has been observed that U-Net based architectures perform better in identifying the exact shape of aneurysms compared to other methods.

In our experiments, we observe that the automated UIA segmentation methods such as Yunqiao et al. [21], Attention U-Net [23] and ResUNet [24] are effective only in detecting the aneurysm locations but not at the delineation of the actual boundary, while the other methods such as Di Noto et al. [20], and Stember et al, [17] are sensitive to the method parameters, thus lacking generalizability. One of the important goals of UIA segmentation is to accurately segment the aneurysm for further follow-up treatment protocols. Our analysis demonstrates that for clinical applications, the most significant metrics for selecting an automated segmentation method are: high recall rate and DSC, followed by high precision. The nnU-Net [29] architecture exhibits better performance in 3D U-Net training and it outperforms Di Noto et al [23] in terms of DSC and volumetric similarity.

TABLE 1. Precision, recall, DSC, IoU, VS and MHD of SOTA methods of SOTA methods.

Sl. No	Method	Mode	Precision	Recall	DSC	IoU	VS	MHD	Rank
1	U-Net [18]	2D	0.7768	0.7775	0.6325	0.5125	0.2	15.02	11
2	Stember et al [17]	2D	0.7797	0.7587	0.6484	0.6209	0.31	12.14	8
3	Sichterrmann et al [19]	2D	0.7787	0.7719	0.6285	0.6069	0.24	15.67	10
4	Yunqiao et al [24]	3D	0.7835	0.7995	0.6734	0.6290	0.38	8.12	3
5	Di Noto et al [23]	3D	0.8084	0.8130	0.6753	0.6405	0.4	6.31	2
6	Claux et al [22]	3D	0.8042	0.6892	0.6521	0.6305	0.27	5.62	4
7	Attention U-Net [25]	2D	0.7867	0.7567	0.6672	0.6325	0.25	9.67	5
8	ResUNet [26]	2D	0.7565	0.7067	0.6588	0.6301	0.28	10.13	6
9	ResUNet++ [27]	2D	0.7145	0.7000	0.6213	0.6194	0.23	12.05	7
10	SegAN [28]	2D	0.7713	0.7010	0.6313	0.6089	0.34	11.27	9
11	nnU-Net[29]	3D	0.8371	0.8051	0.7070	0.6828	0.50	8.96	1

TABLE 2. Precision, recall, DSC, IoU, VS and MHD of SOTA methods (of MIP representation).

Sl. No	Method	Mode	Precision	Recall	DSC	IoU	VS	MHD	Rank
1	U-Net [18]	2D	0.8068	0.7735	0.6751	0.6780	0.2	15.02	2
2	Stember et al [17]	2D	0.8097	0.8003	0.6839	0.6827	0.42	8.67	1
3	Attention U-Net [25]	2D	0.7823	0.7714	0.6506	0.6508	0.3967	6.88	4
4	ResUNet [26]	2D	0.7791	0.7783	0.6512	0.6456	0.2548	7.13	3
5	ResUNet++ [27]	2D	0.7807	0.7029	0.6400	0.6242	0.2124	6.12	5
6	SegAN [28]	2D	0.7813	0.7016	0.6323	0.6089	0.2712	6.58	6

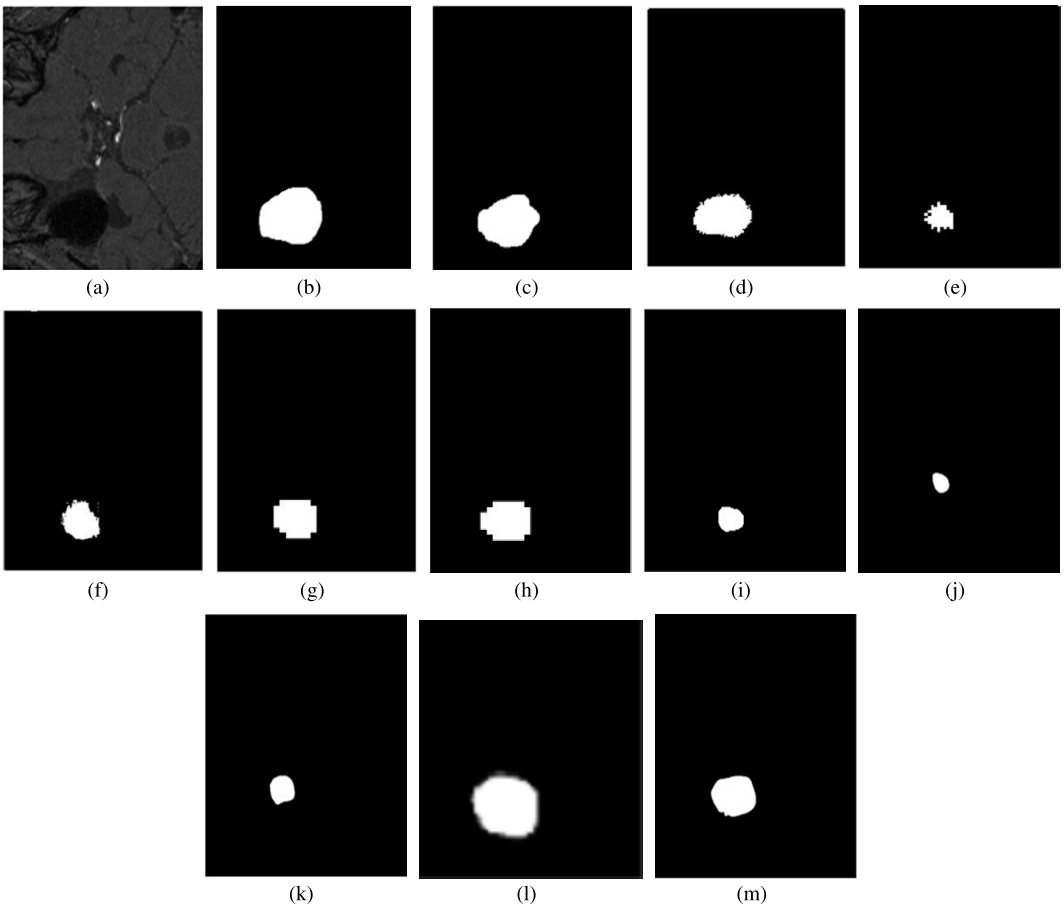

FIGURE 4. Results of different automated unruptured intracranial aneurysm segmentation methods on TOF-MRA scans (a) Original TOF-MRA scan (b) Ground Truth (c) U-Net [18] (d) Stember [17] (e) Sichterrmann [19] (f) Yunqiao [24] (g) Dinoto [23] (h) Claux [22] (i) Attention U-Net [25] (j) ResUNet [26] (k) ResUNet++ [27] (l) SegAN [28] (m) nnU-Net [29].

From the analysis, it is clear that the 3D U-Net generally performs better than the 2D U-Net for image segmentation tasks, especially for tasks that require capturing long-range contextual dependencies. The 3D U-Net architecture is capable of learning spatial relationships between voxels in all three dimensions, while 2D U-Net can only learn spatial

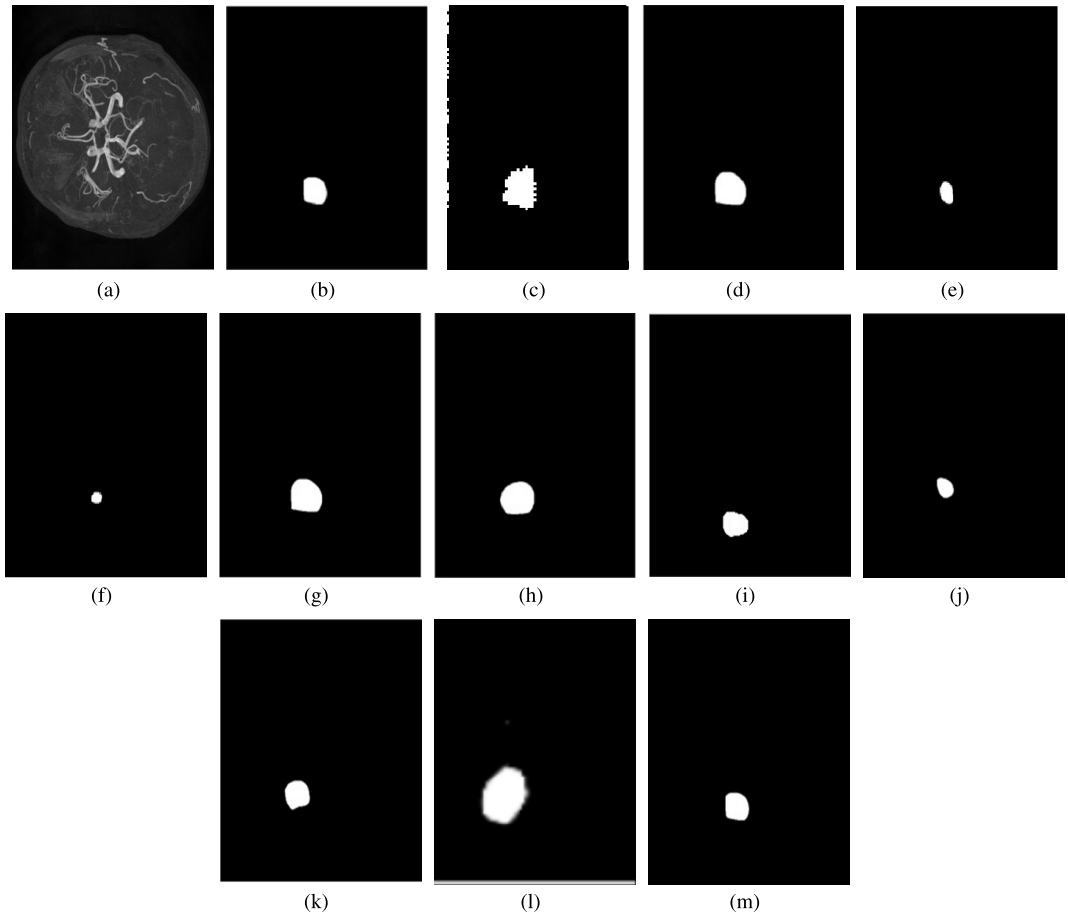

FIGURE 5. Results of different automated unruptured intracranial aneurysm segmentation methods on TOF-MRA scans (a) Original TOF-MRA scan (b) Ground Truth (c) U-Net [18] (d) Stember [17] (e) Sichterrmann [19] (f) Yunqiao [24] (g) Di Noto [23] (h) Claux [22] (i) Attention U-Net [25] (j) ResUNet [26] (k) ResUNet++ [27] (l) SegAN [28] (m) nnunet [29].

relationships between pixels in two dimensions. But the 3D architecture demands high computational and memory requirements to train the model. It also require large amount of data to converge the model without overfitting. Table 3 represents the computational parameters of the existing segmentation methods described in the study. From Table 3, it has been observed that the 2D models such as U-Net [18], Stember et al [17], Attention U-Net [25], ResUNet [26] and ResUNet++ [27] have less computational requirements compared to the 3D models like Sichtermann et al. [19], Di Noto et al. [23], Claux et al. [22] and Yunqiao et al [24].

Overall, 3D U-Net is a good choice for medical image segmentation tasks where accuracy is more important than speed and computational cost.

Some of the reasons behind why 3D U-Net requires more computational resources than 2D U-Net is listed below:

- More Parameters.
- More Computations per pixel.
- Larger input images.

The choice between 2D and 3D approaches depends on factors like the available computational resources and the level of segmentation accuracy required. Additionally, training deep learning models, irrespective of their dimensionality, can be resource-intensive due to the nature of deep learning and the need for ample data and computational power.

In terms of UIA segmentation from TOF-MRA images, the existing methods are subject to certain qualitative constraints. Addressing these limitations in future research has the potential to significantly enhance the precision of UIA segmentation and improve diagnostic capabilities for brain aneurysms. Therefore, it is essential to identify and overcome these constraints in order to further advance the field of UIA segmentation and ultimately improve patient outcomes.

The codes are available at https://github.com/Animaarjun/UIA-segmentation

V. OBSERVATIONS

After comparing various methods, it has been observed that deep neural network architectures exhibit good performance in biomedical segmentation tasks. Out of these architectures, the U-Net based architecture stands out as the most suitable option for aneurysm segmentation tasks, owing to its encoder-decoder structure. However, while existing U-Net architectures are proficient at segmenting aneurysms from TOF-MRA sequences, they do have some shortcomings that can impact the overall efficiency of CAD systems. Therefore,

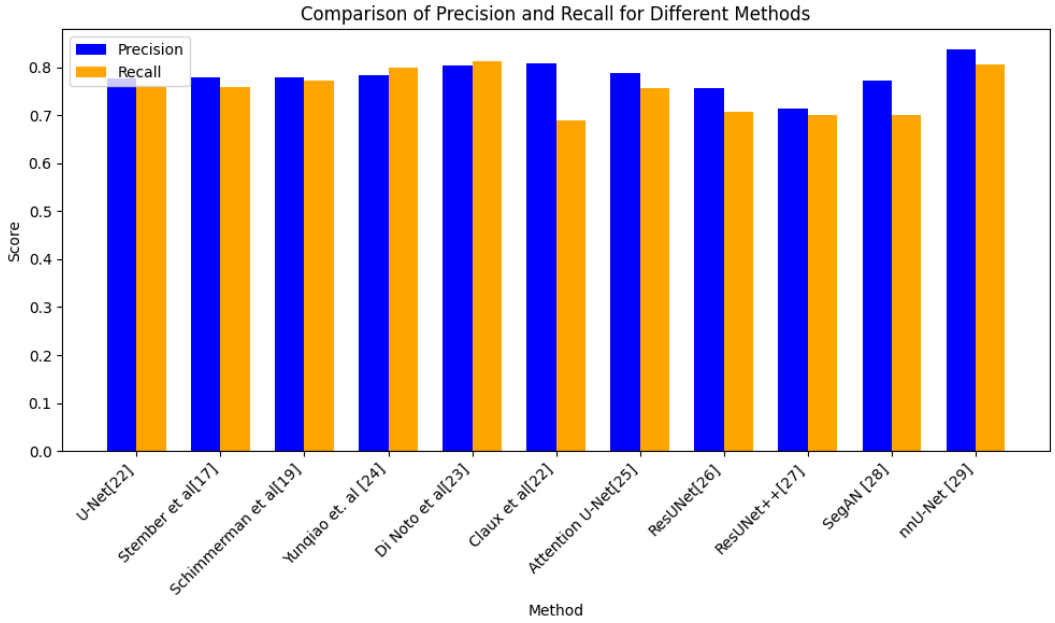

FIGURE 6. Precision and recall plot of the existing UIA and deep learning segmentation methods.

TABLE 3. Hyper parameters of the existing methods.

Sl. No	Paper	Architecture	Model input	Parameters
1	U-Net [18]	U-Net	2D	31043521
2	Stember et al [17]	U- Net	2D	3734513
3	Sichterrmann et al [19]	CNN	3D	11764608
4	Yunqiao et al [24]	3U-Net Ensemble	3D	44705377
5	Di Noto et al [23]	3D U-Net + weak labels	3D	78284619
6	Claux et al [22]	Two stage regularized U-Net	3D	41177649
7	Attention U-Net [25]	U-Net+ attention module	2D	32085765
8	ResUNet [26]	U-Net + residual block	2D	85417713
9	ResUNet++ [27]	U-Net + residual connections	2D	16161772
10	SegAN[28]	FCN + CNN	2D	24432264
11	nnU-Net[29]	nnU-Net	3D	30030423

there is a need for the development of new models for aneurysm detection that ensure the performance efficiency and accuracy of CAD systems in the clinical domain. Based on the comparative analysis, some research gaps have been identified in existing CAD systems. The following observations have been articulated from the comparative analysis.

1) The detection and segmentation of small-sized aneurysms pose a challenge for current architectures, potentially resulting in under detection that can impact the effectiveness of CAD systems in routine clinical settings. The detection and segmentation of small-sized aneurysms can be enhanced by integrating attention mechanisms, such as spatial attention, into deep learning models. These mechanisms enable the model to explicitly focus on the feature descriptors of small-sized aneurysms. Additionally, employing 3D U-Nets with varying patch sizes or multi-resolution convolutional neural networks can further improve the model's capability to learn weak signals from small aneurysms.
2) While the existing CAD system can effectively identify large-sized aneurysms, they occasionally stumble to accurately determining the precise shape and morphological characteristics of the identified aneurysm. While this information is vital in establishing the appropriate treatment plan for those affected. To precisely determine the shape and morphological attributes of aneurysms, the model should integrate shape-related information such as aneurysm volume, neck diameter, sacculation ratio, and wall thickness into the learning process. By doing so, objective measurements can be obtained for characterizing the morphology of aneurysms, thereby aiding in treatment decisions.
3) From this study, we understand that accurately segmenting aneurysms of various sizes and shapes is imperative for assessing the rupture risk of unruptured intracranial aneurysms. The shape and morphological characteristics of the aneurysm structure are closely related to rupture risk estimation, underscoring the importance of precision in segmentation.

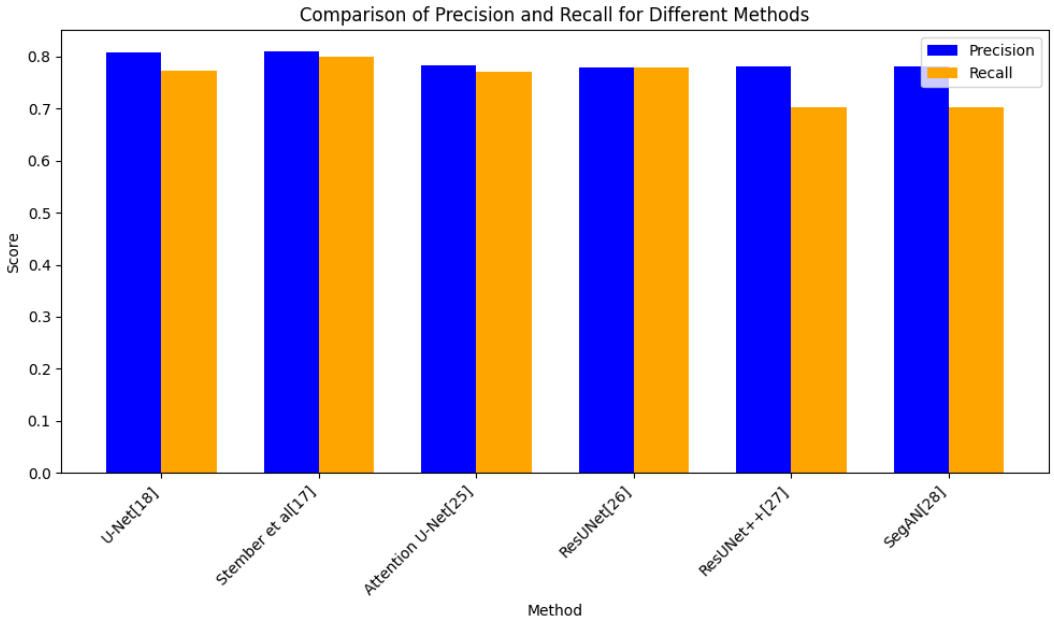

FIGURE 7. Precision and recall plot of the existing UIA and deep learning segmentation methods of MIP representation.

4) Existing 2D U-Net architectures sometimes fail to adequately capture the topological information between different slices of TOF-MRA volume and independently consider the individual slices for detection and segmentation tasks. It may also affect the efficiency and accuracy of CAD models. It demands a CAD model that combines topological and spatial information of the TOF-MRA sequence to develop a model. The current 2D architectures suffer from a lack of 3D context, resulting in the neglect of vital information regarding the overall shape of aneurysms and their relationship with surrounding vessels. By employing 3D convolutions instead of 2D convolutions, the 2D U-Net model can directly capture spatial relationships between slices, addressing this limitation. Additionally, multi-resolution architectures can efficiently capture both fine details within slices and large-scale anatomical relationships across slices. Incorporating attention mechanisms can further enhance segmentation accuracy by highlighting relevant features and suppressing irrelevant ones, thus improving the focus on the aneurysm.
5) The encoder-decoder structure of the U-Net model may lead to overfitting of the models. Thus, it demands either huge training samples or some regularization techniques. But in the medical domain, one major issue is the availability of appropriate training data that helps to generalize the models. So to develop an efficient CAD model, the data scarcity problem needs to be addressed. The scarcity of medical data can be addressed by implementing patch-based augmentation strategies that focus on extracting and augmenting patches containing aneurysms. Additionally, the utilization of Generative Adversarial Networks (GANs) can facilitate the generation of synthetic medical images, effectively augmenting the training datasets and mitigating overfitting within the encoder-decoder structure of U-Net. Employing weakly supervised learning approaches offers another avenue to tackle overfitting issues associated with the U-Net architecture. Furthermore, leveraging pre-trained models on large image datasets with similar features can serve to initialize the deep learning model effectively. Incorporating regularization techniques such as dropout, data augmentation, weight decay, and L1 or L2 regularization can also play a significant role in reducing overfitting.
6) The existing segmentation models are heavily weighted, always demanding high computational requirements. This indicates the requirement for a lightweight model in the aneurysm detection and segmentation task. We can develop a lightweight model by minimizing the number of layers necessary to extract relevant features for segmentation. Additionally, employing techniques such as parameter pruning and quantization can effectively remove redundant features, thereby reducing computational costs. Furthermore, incorporating factored convolutions can be beneficial in further reducing the computational burden.The performance of heavily weighted segmentation models highly depend on large amounts of labelled data. This may lead to bias, and overfitting of the trained model which may pose significant challenges in cerebral aneurysm segmentation task. In order to overcome this, we can use data scarcity methods like semi-supervised learning, data augmentation and the pre-trained models for effective learning.

Based on the identified research gaps in unruptured intracranial aneurysm (UIA) segmentation using deep learning models, researchers can explore semi-supervised learning approaches such as graph-based methods or Generative Adversarial Networks (GANs) to generate synthetic UIA images with diverse shapes and sizes. Additionally, leveraging techniques like deep image prior augmentation and transfer learning can enhance model development. Integration of multi-modal approaches and clinical information, such as patient history and risk markers, into deep learning models can further improve training effectiveness. Through the exploration of these techniques and algorithms, future research aims to construct robust, data-efficient, and interpretable UIA segmentation systems, with the ultimate goal of advancing diagnosis, treatment planning, and patient care for individuals with UIAs.

Before implementing a UIA segmentation system in real-world clinical environments, it is imperative to evaluate its generalizability and effectiveness. This evaluation necessitates preparing the data to mirror real-world scenarios accurately. For 3D data, we create patches sized $64 \times 64 \times 64$, yielding 7,000 samples. Meanwhile, for 2D data, we produce Maximum Intensity Projection (MIP) representations of the volume, resulting in patches of size 64×64 and yielding 4,000 samples. Through assessing state-of-the-art (SOTA) models on these meticulously prepared datasets, we can ascertain the system's adaptability to real-world clinical data.

In addition to UIA segmentation, the system has the capability to analyze cerebral aneurysms by assessing factors such as size, shape, and neck characteristics, along with analyzing hemodynamic flow patterns. It can extend its utility to vascular segmentation and analysis, encompassing structures like carotid arteries and the circle of Willis. Furthermore, the system is adept at segmenting and characterizing brain conditions. Its seamless integration into existing radiological and clinical workflows can be facilitated through either plugin integration or a cloud-based platform. By providing quantitative measurements of parameters like lesion size, volume, and location, the system can contribute valuable data for treatment planning and monitoring disease progression.

VI. CONCLUSION

In our article, we conducted a comprehensive analysis of different automated methods for segmenting unruptured intracranial aneurysms (UIAs) in TOF-MRA scans. Our study employed standardized methodological components and segmentation experiments to highlight the impact of factors like pixel intensity variations, blood vessel shadows, and noise on the accuracy of UIA segmentation.

For an effective UIA segmentation technique, it is essential to be resilient against the aforementioned factors while achieving precise identification and delineation of aneurysms with minimal errors. In our research, we compared the performance of various automated deep learning approaches using TOF-MRA images from the ADAM dataset. We conducted a thorough quantitative and qualitative assessment of the results of UIA segmentation. Our findings revealed that deep neural network architectures outperformed traditional methods. From the quantitative and qualitative analysis, we observed that the 3D U-Net inspired architecture proposed by Di Noto et al [23] and the nnU-Net [29] framework outperforms other methods in terms of the evaluation metrics discussed.

Our future research endeavors will concentrate on refining these algorithms and leveraging deep learning techniques to construct a robust supervised UIA segmentation system. This system will efficiently distinguish between aneurysm and non-aneurysm pixels, thereby enhancing the accuracy of UIA segmentation.

ACKNOWLEDGMENT

The research work is supported by the Kerala State Higher Education Council (KSHEC) under the Kairali Research Award 2020 Project. (File No: KSHEC-A3/352/Kairali Research Award/47/2022).

REFERENCES

[1] A. Keedy, "An overview of intracranial aneurysms," *McGill J. Med.*, vol. 9, no. 2, pp. 141–146, Dec. 2006.
[2] P. M. White, E. M. Teasdale, J. M. Wardlaw, and V. Easton, "Intracranial aneurysms: CT angiography and MR angiography for detection—Prospective blinded comparison in a large patient cohort," *Radiology*, vol. 219, no. 3, pp. 739–749, Jun. 2001, doi: 10.1148/radiology.219.3.r01ma16739.
[3] M. H. Vlak, A. Algra, R. Brandenburg, and G. J. Rinkel, "Prevalence of unruptured intracranial aneurysms, with emphasis on sex, age, comorbidity, country, and time period: A systematic review and meta-analysis," *Lancet Neurol.*, vol. 10, no. 7, pp. 626–636, Jul. 2011.
[4] R. D. Brown and J. P. Broderick, "Unruptured intracranial aneurysms: Epidemiology, natural history, management options, and familial screening," *Lancet Neurol.*, vol. 13, no. 4, pp. 393–404, Apr. 2014.
[5] M. Okahara, H. Kiyosue, M. Yamashita, H. Nagatomi, H. Hata, T. Saginoya, Y. Sagara, and H. Mori, "Diagnostic accuracy of magnetic resonance angiography for cerebral aneurysms in correlation with 3D–Digital subtraction angiographic images: A study of 133 aneurysms," *Stroke*, vol. 33, no. 7, pp. 1803–1808, Jul. 2002.
[6] Z. Shi, B. Hu, U. J. Schoepf, R. H. Savage, D. M. Dargis, C. W. Pan, X. L. Li, Q. Q. Ni, G. M. Lu, and L. J. Zhang, "Artificial intelligence in the management of intracranial aneurysms: Current status and future perspectives," *Amer. J. Neuroradiology*, vol. 41, no. 3, pp. 373–379, Mar. 2020.
[7] K. M. Timmins, "Comparing methods of detecting and segmenting unruptured intracranial aneurysms on TOF-MRAS: The Adam challenge," *NeuroImage*, vol. 238, Sep. 2021, Art. no. 118216.
[8] M. Din, S. Agarwal, M. Grzeda, D. A. Wood, M. Modat, and T. C. Booth, "Detection of cerebral aneurysms using artificial intelligence: A systematic review and meta-analysis," *J. NeuroInterventional Surgery*, vol. 15, no. 3, pp. 262–271, Mar. 2023.
[9] A. M. H. Sailer, B. A. J. M. Wagemans, P. J. Nelemans, R. de Graaf, and W. H. van Zwam, "Diagnosing intracranial aneurysms with MR angiography: Systematic review and meta-analysis," *Stroke*, vol. 45, no. 1, pp. 119–126, Jan. 2014.
[10] Ž. Bizjak and Ž. Špiclin, "A systematic review of deep-learning methods for intracranial aneurysm detection in CT angiography," *Biomedicines*, vol. 11, no. 11, p. 2921, Oct. 2023.
[11] A. Firouzian, R. Manniesing, Z. H. Flach, R. Risselada, F. van Kooten, M. C. J. M. Sturkenboom, A. van der Lugt, and W. J. Niessen, "Intracranial aneurysm segmentation in 3D CT angiography: Method and quantitative validation with and without prior noise filtering," *Eur. J. Radiol.*, vol. 79, no. 2, pp. 299–304, Aug. 2011.
[12] E. Bogunović, J. M. Pozo, M. C. Villa-Uriol, C. B. L. M. Majoie, R. van den Berg, H. A. F. Gratama van Andel, J. M. Macho, J. Blasco, L. San Román, and A. F. Frangi, "Automated segmentation of cerebral vasculature with aneurysms in 3DRA and TOF-MRA using geodesic active regions: An evaluation study," *Med. Phys.*, vol. 38, no. 1, pp. 210–222, Jan. 2011.

[13] Y. Sen, Y. Qian, A. Avolio, and M. Morgan, "Development of image segmentation methods for intracranial aneurysms," *Comput. Math. Methods Med.*, vol. 2013, pp. 1–7, May 2013.
[14] T. F. Chan and L. A. Vese, "Active contours without edges," *IEEE Trans. Image Process.*, vol. 10, no. 2, pp. 266–277, 2001.
[15] S. Suniaga, R. Werner, A. Kemmling, M. Groth, J. Fiehler, and N. D. Forkert, "Computer-aided detection of aneurysms in 3D time-of-flight MRA datasets," in *Proc. 3rd Int. Workshop Mach. Learn. Med. Imag. (MLMI)* (Lecture Notes in Computer Science (Including Subseries Lecture Notes in Artificial Intelligence and Lecture Notes in Bioinformatic)), vol. 7588. Nice, France: Springer, Oct. 2012, pp. 63–69.
[16] X. Yang, D. J. Blezek, L. T. E. Cheng, W. J. Ryan, D. F. Kallmes, and B. J. Erickson, "Computer-aided detection of intracranial aneurysms in MR angiography," *J. Digit. Imag.*, vol. 24, no. 1, pp. 86–95, Feb. 2011, doi: 10.1007/s10278-009-9254-0.
[17] J. N. Stember, P. Chang, D. M. Stember, M. Liu, J. Grinband, C. G. Filippi, P. Meyers, and S. Jambawalikar, "Convolutional neural networks for the detection and measurement of cerebral aneurysms on magnetic resonance angiography," *J. Digit. Imag.*, vol. 32, no. 5, pp. 808–815, Oct. 2019, doi: 10.1007/s10278-018-0162-z.
[18] O. Ronneberger, P. Fischer, and T. Brox, "U-net: Convolutional networks for biomedical image segmentation," in *Proc. Med. Image Comput. Comput.-Assist. Intervent.*, in Lecture Notes in Computer Science, 2015, pp. 234–241, doi: 10.1007/978-3-319-24574-4_28.
[19] T. Sichtermann, A. Faron, R. Sijben, N. Teichert, J. Freiherr, and M. Wiesmann, "Deep learning–based detection of intracranial aneurysms in 3D TOF-MRA," *Amer. J. Neuroradiology*, vol. 40, no. 1, pp. 25–32, Jan. 2019, doi: 10.1007/s10278-018-0162-z.
[20] S. M. Smith, "Fast robust automated brain extraction," *Human Brain Mapping*, vol. 17, no. 3, pp. 143–155, Nov. 2002, doi: 10.1002/hbm.10062.
[21] N. J. Tustison, B. B. Avants, P. A. Cook, Y. Zheng, A. Egan, P. A. Yushkevich, and J. C. Gee, "N4ITK: Improved N3 bias correction," *IEEE Trans. Med. Imag.*, vol. 29, no. 6, pp. 1310–1320, Jun. 2010, doi: 10.1109/TMI.2010.2046908.
[22] F. Claux, M. Baudouin, C. Bogey, and A. Rouchaud, "Dense, deep learning-based intracranial aneurysm detection on TOF MRI using two-stage regularized U-Net," *J. Neuroradiology*, vol. 50, no. 1, pp. 9–15, Feb. 2023, doi: 10.1016/j.neurad.2022.03.005.
[23] T. Di Noto, G. Marie, S. Tourbier, Y. Alemán-Gómez, O. Esteban, G. Saliou, M. B. Cuadra, P. Hagmann, and J. Richiardi, "Towards automated brain aneurysm detection in TOF-MRA: Open data, weak labels, and anatomical knowledge," *Neuroinformatics*, vol. 21, no. 1, pp. 21–34, Jan. 2023, doi: 10.1007/s12021-022-09597-0.
[24] Y. Yang, Y. Lin, Y. Li, D. Wei, K. Ma, X. Yang, and Y. Zheng, "Automatic aneurysm segmentation via 3D U-net ensemble," *Lancet Neurology.*, vol. 7588, no. 7, pp. 63–69, Feb. 2020, doi: 10.1109/ICMA52036.2021.9512662.
[25] O. Oktay, J. Schlemper, L. L. Folgoc, M. Lee, M. Heinrich, K. Misawa, K. Mori, S. McDonagh, N. Y. Hammerla, B. Kainz, B. Glocker, and D. Rueckert, "Attention U-net: Learning where to look for the pancreas," in *Proc. IOOC-ECOC*, Boston, MA, USA, 2018, pp. 585–590.
[26] F. I. Diakogiannis, F. Waldner, P. Caccetta, and C. Wu, "ResUNet—A: A deep learning framework for semantic segmentation of remotely sensed data," *ISPRS J. Photogramm. Remote Sens.*, vol. 162, pp. 94–114, Apr. 2020.
[27] D. Jha, P. H. Smedsrud, M. A. Riegler, D. Johansen, T. D. Lange, P. Halvorsen, and H. D. Johansen, "ResUNet++: An advanced architecture for medical image segmentation," in *Proc. IEEE Int. Symp. Multimedia (ISM)*, Dec. 2019, pp. 225–2255, doi: 10.1109/ISM46123.2019.00049.
[28] Y. Xue, T. Xu, H. Zhang, L. R. Long, and X. Huang, "SegAN: Adversarial network with multi-scale l1 loss for medical image segmentation," *Neuroinformatics*, vol. 16, nos. 3–4, pp. 383–392, Oct. 2018, doi: 10.1007/s12021-018-9377-x.
[29] F. Isensee, P. F. Jaeger, S. A. A. Kohl, J. Petersen, and K. H. Maier-Hein, "NnU-net: A self-configuring method for deep learning-based biomedical image segmentation," *Nature Methods*, vol. 18, no. 2, pp. 203–211, Feb. 2021.
[30] K. Timmins, E. Bennink, I. van der Schaaf, B. Velthuis, Y. Ruigrok, and H. Kuijf, "Intracranial aneurysm detection and segmentation challenge," in *Proc. MICCAI*, 2020, pp. 30–31.
[31] Y. Bengio, I. Goodfellow, and A. Courville, *Deep Learning*, vol. 29. Cambridge, MA, USA: MIT Press, 2016, p. 7553.
[32] A. A. Taha and A. Hanbury, "Metrics for evaluating 3D medical image segmentation: Analysis, selection, and tool," *BMC Med. Imag.*, vol. 88, no. 17, pp. 1600–1606, Dec. 2015.
[33] W. Ji, A. Liu, X. Lv, H. Kang, L. Sun, Y. Li, X. Yang, C. Jiang, and Z. Wu, "Risk score for neurological complications after endovascular treatment of unruptured intracranial aneurysms," *Stroke*, vol. 47, no. 4, pp. 971–978, Apr. 2016, doi: 10.1161/strokeaha.115.012097.
[34] X. Glorot and Y. Bengio, "Understanding the difficulty of training deep feedforward neural networks," *J. Mach. Learn. Res.*, pp. 249–256, 2010.
[35] D. P. Chakraborty and K. S. Berbaum, "Observer studies involving detection and localization: Modeling, analysis, and validation," *Med. Phys.*, vol. 31, no. 8, pp. 2313–2330, Jul. 2004, doi: 10.1118/1.1769352.
[36] J. Frösen, R. Tulamo, A. Paetau, E. Laaksamo, M. Korja, A. Laakso, M. Niemelä, and J. Hernesniemi, "Saccular intracranial aneurysm: Pathology and mechanisms," *Acta Neuropathologica*, vol. 123, no. 6, pp. 773–786, Jun. 2012, doi: 10.1007/s00401-011-0939-3.
[37] B. Rao, V. Zohrabian, P. Cedeno, A. Saha, J. Pahade, and M. A. Davis, "Utility of artificial intelligence tool as a prospective radiology peer reviewer—Detection of unreported intracranial hemorrhage," *Academic Radiol.*, vol. 28, no. 1, pp. 85–93, Jan. 2021, doi: 10.1016/j.acra.2020.01.035.
[38] R. Fardel, M. Nagel, F. Nüesch, T. Lippert, and A. Wokaun, "Fabrication of organic light-emitting diode pixels by laser-assisted forward transfer," *Appl. Phys. Lett.*, vol. 91, no. 6, Aug. 2007, Art. no. 061103.
[39] M. I. Razzak, S. Naz, and A. Zaib, "Deep learning for medical image processing: Overview, challenges and the future," in *Classification in BioApps* (Lecture Notes in Computational Vision and Biomechanics), vol. 26, 2018, pp. 323–350, doi: 10.1007/978-3-319-65981-7_2.
[40] S. A. Taghanaki, Y. Zheng, S. Kevin Zhou, B. Georgescu, P. Sharma, D. Xu, D. Comaniciu, and G. Hamarneh, "Combo loss: Handling input and output imbalance in multi-organ segmentation," *Computerized Med. Imag. Graph.*, vol. 75, pp. 24–33, Jul. 2019.
[41] A. Creswell, T. White, V. Dumoulin, K. Arulkumaran, B. Sengupta, and A. A. Bharath, "Generative adversarial networks: An overview," *IEEE Signal Process. Mag.*, vol. 35, no. 1, pp. 53–65, Jan. 2018.
[42] A. A. Taha and A. Hanbury, "Metrics for evaluating 3D medical image segmentation: Analysis, selection, and tool," *BMC Med. Imag.*, vol. 15, no. 1, pp. 1–28, Dec. 2015.

V. A. ANIMA received the M.Tech. degree in computer science and engineering from the Department of Computer Science and Engineering, National Institute of Technology Karnataka, India, in 2016. She is currently pursuing the Ph.D. degree with Cochin University of Science and Technology, Kochi, Kerala, India. Her research interests include image processing, computer vision, medical image analysis, deep learning, and machine learning.

MADHU S. NAIR (Senior Member, IEEE) received the M.Tech. degree (Hons.) in computer science (with a specialization in digital image computing) from the University of Kerala, in 2008, and the Ph.D. degree in computer science (image processing) from Mahatma Gandhi University, in 2013. He is currently a Professor with the Department of Computer Science, Cochin University of Science and Technology, Kerala, India. His research interests include digital image processing, pattern recognition, computer vision, data compression, and soft computing. He was a recipient of prestigious national awards, such as the AICTE Travel Grant Award, in 2008; the INAE Innovative Student Projects Award for the Best M.Tech. Thesis, in 2009; the CSI Paper Presenter Award at the International Conference; the AICTE Career Award for Young Teachers; the IEI Young Engineers Award, from 2013 to 2014; the SSI Young Systems Scientist Award, in 2015; the IETE-Smt Manorama Rathore Memorial Award, in 2017; the Government of Kerala's Kairali Research Award, in 2020; and the AICTE Visvesvaraya Best Teacher Award, in 2021. He is serving as a reviewer for around 40 international journals published by IEEE, Elsevier, Springer, Wiley, and World-Scientific.